

---

# Tissue transglutaminase modulates $\alpha$ -synuclein oligomerization

---

INE M.J. SEGERS-NOLTEN,<sup>1</sup> MICHA M.M. WILHELMUS,<sup>2</sup> GERTJAN VELDHUIS,<sup>1</sup>  
BART D. VAN ROOIJEN,<sup>1</sup> BENJAMIN DRUKARCH,<sup>2</sup> AND VINOD SUBRAMANIAM<sup>1</sup>

<sup>1</sup>Biophysical Engineering Group, MESA+ Institute for Nanotechnology and Institute for Biomedical Technology, University of Twente, 7500 AE Enschede, The Netherlands

<sup>2</sup>Department of Anatomy and Neurosciences, Institute for Clinical and Experimental Neurosciences (ICEN), VU University Medical Center, Amsterdam, The Netherlands

(RECEIVED April 29, 2008; FINAL REVISION May 22, 2008; ACCEPTED May 22, 2008)

## Abstract

We have studied the interaction of the enzyme tissue transglutaminase (tTG), catalyzing cross-link formation between protein-bound glutamine residues and primary amines, with Parkinson's disease-associated  $\alpha$ -synuclein protein variants at physiologically relevant concentrations. We have, for the first time, determined binding affinities of tTG for wild-type and mutant  $\alpha$ -synucleins using surface plasmon resonance approaches, revealing high-affinity nanomolar equilibrium dissociation constants. Nanomolar tTG concentrations were sufficient for complete inhibition of fibrillization by effective  $\alpha$ -synuclein cross-linking, resulting predominantly in intramolecularly cross-linked monomers accompanied by an oligomeric fraction. Since oligomeric species have a pathophysiological relevance we further investigated the properties of the tTG/ $\alpha$ -synuclein oligomers. Atomic force microscopy revealed morphologically similar structures for oligomers from all  $\alpha$ -synuclein variants; the extent of oligomer formation was found to correlate with tTG concentration. Unlike normal  $\alpha$ -synuclein oligomers the resultant structures were extremely stable and resistant to GdnHCl and SDS. In contrast to normal  $\beta$ -sheet-containing oligomers, the tTG/ $\alpha$ -synuclein oligomers appear to be unstructured and are unable to disrupt phospholipid vesicles. These data suggest that tTG binds equally effectively to wild-type and disease mutant  $\alpha$ -synuclein variants. We propose that tTG cross-linking imposes structural constraints on  $\alpha$ -synuclein, preventing the assembly of structured oligomers required for disruption of membranes and for progression into fibrils. In general, cross-linking of amyloid forming proteins by tTG may prevent the progression into pathogenic species.

**Keywords:**  $\alpha$ -synuclein; tissue transglutaminase; cross-linking; oligomer; surface plasmon resonance; atomic force microscopy; Parkinson's disease

**Supplemental material:** see [www.proteinscience.org](http://www.proteinscience.org)

---

Reprint requests to: Vinod Subramaniam, Biophysical Engineering Group, MESA+ Institute for Nanotechnology and Institute for Biomedical Technology, University of Twente, P.O. Box 217, 7500 AE Enschede, The Netherlands; e-mail: [v.subramaniam@tnw.utwente.nl](mailto:v.subramaniam@tnw.utwente.nl); fax: 31-53-4891105; or Benjamin Drukarch, Department of Anatomy and Neurosciences, Institute for Clinical and Experimental Neurosciences (ICEN), VU University Medical Center, 1081 BT, Amsterdam, The Netherlands; e-mail: [b.drukarch@vumc.nl](mailto:b.drukarch@vumc.nl); fax: 31-20-4448100.

Article and publication are at <http://www.proteinscience.org/cgi/doi/10.1110/ps.036103.108>.

The enzyme tissue transglutaminase (tTG) plays a role in various neurodegenerative diseases (Muma 2007). tTG enzyme activity, catalyzing covalent bond formation between a protein-bound glutamine  $\gamma$ -carboximide group and a primary amino group, such as those present in lysine residues, has been shown to be up-regulated in disease affected brain (Kim et al. 1999). Cytoplasmic inclusions known as Lewy bodies, mainly containing

fibrillar aggregates of  $\alpha$ -synuclein protein, are found in Parkinson's disease (PD)-affected brain neurons (Spillantini et al. 1997). tTG-catalyzed cross-links have been found colocalized with Lewy bodies, suggesting a role for tTG in the pathophysiology of PD (Junn et al. 2003).

tTG may potentiate inter- or intramolecular cross-links or combinations thereof. Cellular and in vitro studies have mainly focused on intermolecular cross-linking of amyloidogenic proteins by tTG, leading to formation of insoluble complexes (Miller and Johnson 1995; Junn et al. 2003). Recently, intramolecularly cross-linked  $\alpha$ -synuclein monomer was discovered to be highly enriched in PD *substantia nigra* tissue relative to control tissue (Andringa et al. 2004). Cross-linked  $\alpha$ -synuclein appeared to correlate with disease progression, indicating that tTG cross-linking may change the structure of monomeric  $\alpha$ -synuclein resulting in altered functionality. In vitro investigations on the effect of tTG demonstrated preferential formation of monomeric intramolecular cross-links at relatively low  $\alpha$ -synuclein concentration (Konno et al. 2005a). At micromolar tTG concentrations, fibrillar aggregation of wild-type  $\alpha$ -synuclein was blocked with little evidence of covalently linked multimers. Only a negligible fraction containing small soluble granules was observed using size-exclusion chromatography (SEC) and transmission electron microscopy. Intramolecular cross-linking by tTG was hypothesized to be protective in PD, by inhibiting the assembly of monomeric  $\alpha$ -synuclein into amyloid fibrils and its potentially toxic oligomeric precursors (Lashuel et al. 2002).

To shed light on the pathological relevance, information on the structural and functional properties of the small granules and cross-linked monomers is required for wild-type and disease mutant  $\alpha$ -synuclein. A merely beneficial role for tTG is hard to claim, because of the observed correlation between intramolecularly cross-linked monomer concentration and disease progression (Andringa et al. 2004), commensurate with enhanced expression of both tTG and  $\alpha$ -synuclein. Hence, the impact of tTG action may depend on  $\alpha$ -synuclein and tTG concentration. Therefore, we have comprehensively and systematically investigated tTG cross-linking of wild-type and disease-related mutant A30P, E46K, and A53T  $\alpha$ -synuclein. We evaluated the effect of physiologically relevant (Murtaugh et al. 1984; Konno et al. 2005b) nanomolar tTG concentrations on cross-linking kinetics, on affected  $\alpha$ -synuclein fraction, and on inhibition of aggregation. Surface plasmon resonance (SPR) measurements revealed high-affinity nanomolar equilibrium dissociation constants of tTG for all  $\alpha$ -synuclein variants. Morphological assessment of tTG/ $\alpha$ -synuclein reaction products with atomic force microscopy (AFM) indicated the formation of very distinct, uniform, oligomeric species. Since oligomeric  $\alpha$ -synuclein structures are now considered as the pathophysiological most relevant structures in PD (Lashuel et al. 2002), we determined

the stability, secondary structure content, foldability, and vesicle permeabilization properties of purified tTG/ $\alpha$ -synuclein oligomers compared to normal oligomers. Our results demonstrate that the extent of tTG/ $\alpha$ -synuclein oligomer formation correlates with tTG concentration, and that all  $\alpha$ -synuclein variants are equally affected by tTG. Unlike normal oligomers found on the pathway to fibril formation, tTG/ $\alpha$ -synuclein oligomers are extremely stable against denaturing conditions, contain no secondary structure, and do not show vesicle permeabilization capability.

## Results

### tTG concentration-dependent cross-linking of $\alpha$ -synuclein

In contrast to an earlier report (Konno et al. 2005a) using micromolar tTG concentrations, we explored the effect of nanomolar tTG concentrations, consistent with cellular tTG levels, on  $\alpha$ -synuclein cross-linking (Murtaugh et al. 1984; Konno et al. 2005b). SDS-PAGE (Fig. 1) shows that at 1 nM tTG nearly all  $\alpha$ -synuclein is contained in a single band, representing non-cross-linked monomeric protein. At higher tTG concentrations a second lower band becomes more intense, indicating an increasing protein fraction with higher gel mobility. The data suggest that intramolecular cross-linking by tTG forces monomeric  $\alpha$ -synuclein protein into a more compact and thus more

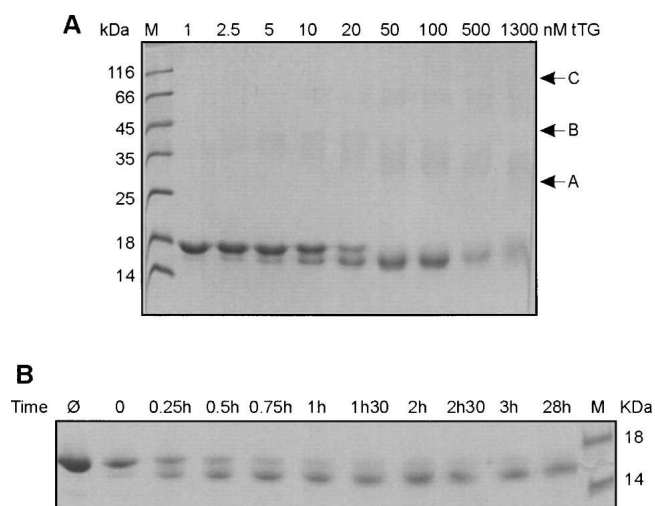


**Figure 1.** tTG concentration-dependent cross-linking of wild-type  $\alpha$ -synuclein. Samples of 100  $\mu$ M  $\alpha$ -synuclein incubated with different tTG concentrations at 37°C for 68 h were loaded on a 16.5% SDS-PAGE gel. (A) Lane M: low molecular mass marker; for the other lanes the tTG concentrations are indicated on the top. Arrows A, B, and C indicate specific gel regions described in the text. (B) SDS-PAGE result of progression of 100  $\mu$ M wild-type  $\alpha$ -synuclein cross-linking with 50 nM tTG. Lane  $\emptyset$ : no tTG added; lane M: low molecular mass marker; for the other lanes the incubation times are indicated on the top. Quantitative analysis is shown in Supplemental Figure S1.

mobile structure. Virtually all  $\alpha$ -synuclein appears to be cross-linked at 50 nM tTG, while with increasing tTG concentrations a slightly increasing amount (up to  $\sim 30\%$  at 1.3  $\mu\text{M}$  tTG) of higher molecular mass material is formed, represented by a faint band between 25 and 45 kDa (between arrows A and B). From 1 nM to 20 nM tTG, this band broadens at the lower side, while above 50 nM tTG a compaction and shift to lower molecular mass positions is evident. We postulate that these bands represent SDS-resistant intermolecularly cross-linked dimeric  $\alpha$ -synuclein, and that higher tTG concentrations cause multiple intramolecular cross-links, resulting in more compaction. An analogous pattern can be observed for higher molecular mass species (between arrows B and C). Discrimination of multiply cross-linked species within the monomeric population is prohibited by the low resolution of the gel. Total protein in the 500 and 1300 nM tTG lanes is reduced to  $\sim 70\%$ , likely due to increased formation of intermolecularly cross-linked higher molecular mass oligomers not able to enter the gel matrix (see also Fig. 3C, lane 4).

We followed the temporal progression of  $\alpha$ -synuclein cross-linking with 50 nM tTG, the concentration just sufficient to cross-link all protein (Fig. 1A), by SDS-PAGE analysis (Fig. 1B). After 1 h the majority of protein is cross-linked, leaving a non-cross-linked fraction of about 30%, while the cross-linking reaction is complete within 2 to 3 h (quantitative analysis in Supplemental Fig. S1).

#### Nanomolar tTG is sufficient to block aggregation of wild-type and disease mutant $\alpha$ -synuclein

The results shown above indicate that tTG effectively cross-links wild-type  $\alpha$ -synuclein at physiologically relevant concentrations of both tTG and of  $\alpha$ -synuclein. We extended the investigation of the cross-linking effect of 50 nM tTG on the aggregation of wild-type  $\alpha$ -synuclein to the known disease mutants. For reference, aggregation reactions were also performed at 1.3  $\mu\text{M}$  tTG, consistent with a previous study performed on the wild-type protein (Konno et al. 2005a). Aggregate formation was monitored by binding of the  $\beta$ -sheet specific fluorescent dye Thioflavin T (ThioT). The left panel of Figure 2 depicts typical examples of aggregation curves in the presence and absence of tTG. In the absence of tTG typical aggregation kinetics were observed with half-times for wild-type and A30P of 90 h and 50 h, respectively, and for E46K and A53T of 25 h. The complete absence of ThioT intensity in the presence of 50 nM and 1.3  $\mu\text{M}$  tTG over the full time course of the reaction for all  $\alpha$ -synuclein variants clearly indicates that wild-type and disease mutants of  $\alpha$ -synuclein are equally affected by tTG regarding  $\beta$ -sheet formation.

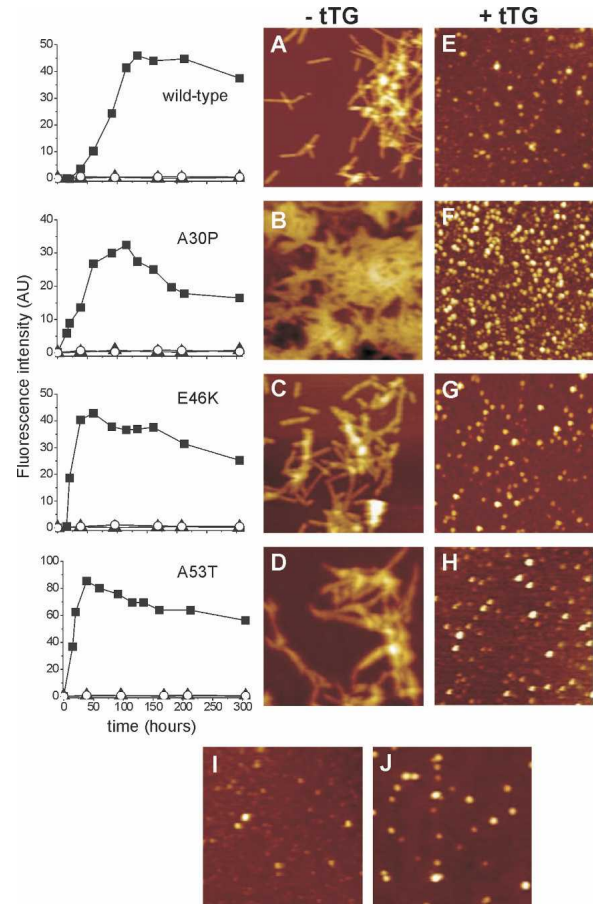


**Figure 2.** Aggregation of  $\alpha$ -synuclein variants in the presence and absence of tTG. (Left panel) ThioT fluorescence assay. Wild-type, A30P, E46K, and A53T  $\alpha$ -synuclein were incubated at a concentration of 100  $\mu\text{M}$  without (filled squares), and with 50 nM (filled triangles) and 1.3  $\mu\text{M}$  tTG (open circles). (Right panel) AFM images of  $\alpha$ -synuclein aggregation products in the final plateau phase of the Thio T curves. (Left column) In the absence of tTG for wild-type, A30P, E46K, and A53T  $\alpha$ -synuclein (A, B, C, and D, respectively). (Right column) After incubation of wild-type, A30P, E46K, and A53T  $\alpha$ -synuclein with 1.3  $\mu\text{M}$  tTG (E, F, G, and H, respectively). Image I is a representative example of 100  $\mu\text{M}$  wild-type  $\alpha$ -synuclein incubated with 50 nM tTG. Image J: normal wild-type  $\alpha$ -synuclein oligomers without tTG. All images are  $1.25 \times 1.25 \mu\text{m}^2$ .

#### AFM reveals $\alpha$ -synuclein oligomers as end products of tTG interaction

The ThioT data (Fig. 2) indicate that no  $\beta$ -sheet structures are formed in  $\alpha$ -synuclein in the presence of tTG, probably implying the exclusion of fibril formation. We performed AFM imaging to visualize the morphology of the structures formed in the absence and presence of nM and  $\mu\text{M}$  tTG concentrations (Fig. 2). In the absence of tTG, AFM images clearly show the presence of fibrillar structures for all  $\alpha$ -synuclein variants. In the presence of tTG, however, only small round features are present (Fig. 2E–H) which resemble the oligomeric intermediates

normally formed on the aggregation pathway (Fig. 2J). All  $\alpha$ -synuclein variants exhibit similar morphologies upon incubation with either 50 nM or 1.3  $\mu$ M tTG with average measured oligomer heights of  $4.9 \pm 1.5$  nm ( $n = 100$ ), while normal oligomers formed in the absence of tTG are  $4.5 \pm 1.0$  nm high ( $n = 100$ ).

#### Equal binding affinity of tTG for all $\alpha$ -synuclein variants

tTG inhibits fibril formation for wild-type  $\alpha$ -synuclein and the disease mutants A30P, E46K, and A53T equally well, indicating that the mutations do not significantly alter the binding specificity of tTG. SPR measurements confirmed these results, yielding high association and low dissociation of tTG from the sensor chip coated with  $\alpha$ -synuclein variants. Analysis of the data revealed nanomolar equilibrium dissociation constants ( $K_D$ ), indicating high-affinity binding of  $\alpha$ -synuclein to tTG (Table 1), without significant difference between  $\alpha$ -synuclein variants.

#### Oligomers constitute only a fraction of the total tTG/ $\alpha$ -synuclein reaction

The AFM images suggest that oligomers are the predominant species formed in the presence of tTG under aggregation promoting conditions. The resolution of the AFM technique is, however, not sufficient to resolve monomeric  $\alpha$ -synuclein or protein assemblies containing only a few monomers. SEC analysis of the  $\alpha$ -synuclein/tTG reactions (Fig. 3A) revealed that oligomers, eluting at about 8 mL, only constitute a minor fraction of the total reaction product of 1.3  $\mu$ M tTG-treated  $\alpha$ -synuclein. The majority consists of apparently intramolecularly cross-linked monomers, eluting slightly later (at 14.6 mL) than untreated monomers (at 14.2 mL). This observation is consistent with the faster migration of tTG cross-linked  $\alpha$ -synuclein monomers observed in SDS-PAGE (Fig. 1). Moreover, SDS-PAGE analysis of 1.3  $\mu$ M tTG/ $\alpha$ -synuclein samples (Fig. 1) indicated that  $\sim 30\%$  of protein formed oligomeric structures too large to enter the gel matrix. Size-exclusion analysis corroborates this observation revealing an equal 30% fraction eluting in the higher mass region at volumes smaller than 12 mL. Native PAGE confirms that smaller assemblies of  $\alpha$ -synuclein, possibly dimers, trimers, tetramers (peak at  $\sim 12.8$  mL), and monomers, are

**Table 1.** Equilibrium dissociation constants (mean  $\pm$  SE) for binding of wild-type, A30P, E46K, and A53T  $\alpha$ -synuclein to tTG

| $\alpha$ -Synuclein | Wild type     | A30P          | E46K          | A53T          |
|---------------------|---------------|---------------|---------------|---------------|
| $K_D$ (nM)          | $4.7 \pm 1.3$ | $2.2 \pm 0.2$ | $2.7 \pm 0.5$ | $5.2 \pm 5.1$ |

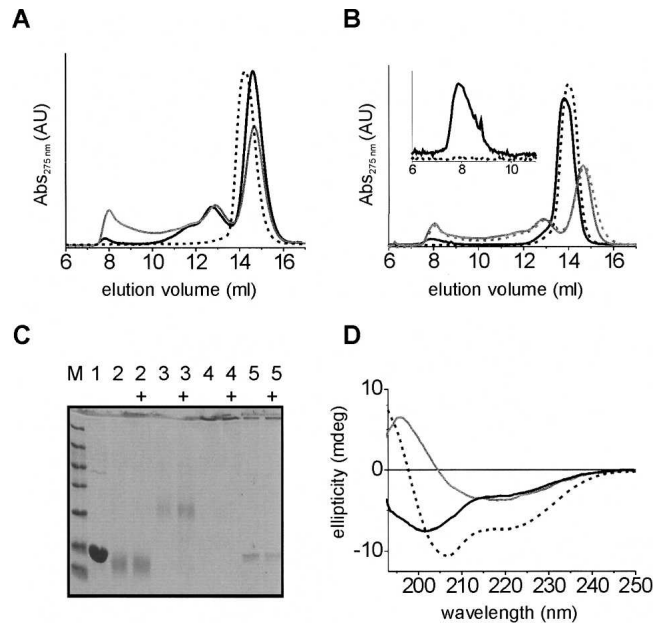


**Figure 3.** Characterization of tTG/ $\alpha$ -synuclein oligomers. (A) SEC analysis of tTG/ $\alpha$ -synuclein reactions with 50 nM (black solid) and 1.3  $\mu$ M tTG (gray) for 158 h at 37°C; normal monomers (black dashed line). (B) Samples from A without (solid) or with (dashed) 5 M GdnHCl treatment for 30 min at room temperature; gray profiles: 1.3  $\mu$ M tTG samples from A; black profiles: normal  $\alpha$ -synuclein oligomers; (inset) zoom-in on normal oligomer peak eluting at  $\sim 8$  mL. All profiles in A and B normalized on area. (C) Fifteen percent SDS-PAGE gel of 1.3  $\mu$ M tTG/ $\alpha$ -synuclein fractions from SEC (A) and comparison with normal  $\alpha$ -synuclein monomers and oligomers. Lane M, low molecular mass marker; lane 1, untreated monomers; lane 2,  $\sim 14.6$  mL monomeric tTG/ $\alpha$ -synuclein fraction; lane 3,  $\sim 12.9$  mL intermediate tTG/ $\alpha$ -synuclein fraction; lane 4,  $\sim 8$  mL oligomeric tTG/ $\alpha$ -synuclein fraction; lane 5, normal oligomers. Samples with “+” were heated for 5 min at 95°C before loading. (D) CD spectra of tTG/ $\alpha$ -synuclein oligomers and normal  $\alpha$ -synuclein oligomers. Black spectra: oligomeric tTG/ $\alpha$ -synuclein, SEC fraction eluting at  $\sim 8$  mL, before (solid line) and after (dashed line) addition of 0.1% (w/v) SDS. Gray spectrum: normal  $\alpha$ -synuclein oligomers.

indeed found at volumes larger than 12 mL (Supplemental Fig. S2). With 50 nM tTG the oligomeric fraction is smaller than with 1.3  $\mu$ M tTG, indicating tTG concentration-dependent oligomer formation. Identical results were obtained for all  $\alpha$ -synuclein variants.

Oligomeric species are thought to be relevant for the pathophysiology of the disease. We therefore characterized the biophysical properties, such as stability, secondary structure content, foldability, and vesicle permeabilization capability of the tTG/ $\alpha$ -synuclein oligomers and compared them to normal oligomers. Because of the low oligomer yield from 50 nM tTG reactions, we used purified tTG/ $\alpha$ -synuclein oligomers generated from a reaction using 1.3  $\mu$ M tTG. These results are considered to be representative for tTG/ $\alpha$ -synuclein oligomers, based on comparable ThioT signals, similar oligomer morphology,

and SEC elution at both micro- and nanomolar concentrations (Figs. 2, 3).

#### *tTG/ $\alpha$ -synuclein oligomers are extremely stable*

We tested the stability of the tTG/ $\alpha$ -synuclein oligomers in the presence of 5 M GdnHCl. SEC clearly showed that the tTG/ $\alpha$ -synuclein oligomers were not disrupted by the harsh GdnHCl treatment (Fig. 3B, gray), in contrast to normal oligomers that do fall apart (Fig. 3B, black + inset). This result indicates that the tTG/ $\alpha$ -synuclein oligomers are indeed stabilized by covalent intermolecular bonds. Additionally, we tested the resistance of tTG/ $\alpha$ -synuclein oligomers to SDS. SDS-PAGE analysis (Fig. 3C) shows no dissociation into monomers of the tTG/ $\alpha$ -synuclein oligomers and the intermediate fractions, demonstrating their stability to SDS treatment and heating. The band at the interface between stacking and separating gel indicates that apparently the intact tTG/ $\alpha$ -synuclein oligomers cannot enter the separating gel. Normal oligomers, however, are only partially resistant to SDS, as demonstrated by the appearance of a monomer band. The combined data indicate that tTG/ $\alpha$ -synuclein oligomers are stabilized by covalent intermolecular bonds formed by tTG.

#### *tTG/ $\alpha$ -synuclein oligomers do not contain $\beta$ -sheet structure*

We investigated the secondary structure of the tTG/ $\alpha$ -synuclein oligomers by CD spectroscopy. The CD spectrum of the SEC purified tTG/ $\alpha$ -synuclein oligomers (Fig. 3D) resembles mostly a random coil spectrum in contrast to the  $\beta$ -sheet containing structure of normal wild-type oligomers, indicating that the tTG/ $\alpha$ -synuclein oligomers are different molecular architectures than normal oligomers. Surprisingly, 0.1% SDS still renders the unstructured tTG/ $\alpha$ -synuclein oligomers into  $\alpha$ -helix conformation, indicating that the tTG cross-links do not impede folding of the N-terminal domain. tTG/ $\alpha$ -synuclein monomers, like normal monomers, do not exhibit secondary structure, but form  $\alpha$ -helix in the presence of SDS (Supplemental Fig. S3).

#### *tTG/ $\alpha$ -synuclein oligomers are not able to disrupt lipid vesicles*

The oligomeric structures transiently occurring during normal aggregation of  $\alpha$ -synuclein into fibrils have been shown to permeabilize and disrupt lipid vesicles (Volles et al. 2001). The CD and stability data clearly indicate that tTG-induced  $\alpha$ -synuclein oligomers are structurally different from normal oligomers. To investigate if tTG/ $\alpha$ -synuclein oligomers are also functionally different, a calcein dye efflux assay was performed on POPG (1-palmitoyl, 2-oleoyl phosphatidylglycerol) LUVs (large

unilamellar vesicles) using SEC purified tTG/ $\alpha$ -synuclein oligomers. The results clearly show that tTG/ $\alpha$ -synuclein oligomers and monomers do not disrupt lipid vesicles at any of the concentrations tested (Fig. 4). This observation is in stark contrast to the effect of purified normal oligomers of wild-type  $\alpha$ -synuclein that cause >80% permeabilization at 1  $\mu$ M.

## Discussion

We have shown that nanomolar tTG concentrations are sufficient to completely cross-link 100  $\mu$ M monomeric wild-type and disease-mutant  $\alpha$ -synuclein. The ThioT results reflect the extremely high effectiveness of tTG, that is, nanomolar concentrations are sufficient to prevent formation of  $\beta$ -sheet-rich amyloid aggregates over a prolonged time span. The data indicate that tTG is able to effectively inhibit  $\alpha$ -synuclein aggregation even at concentrations two to three orders of magnitude lower than those previously reported (Konno et al. 2005a). In combination with the SDS-PAGE data, this observation suggests that the primarily intramolecular cross-links formed at nanomolar tTG concentrations obstruct the folding of  $\alpha$ -synuclein into the  $\beta$ -sheet conformations that are predominant in amyloid species. Fast formation of intramolecular cross-links in  $\alpha$ -synuclein may thus be a way to prevent formation of pathogenic structures.

AFM clearly identified characteristic oligomeric structures for all  $\alpha$ -synuclein variants. At this stage it is not clear which of the six glutamine residues in  $\alpha$ -synuclein are involved in the cross-linking reaction by tTG. It is possible that only some of the six glutamine residues in  $\alpha$ -synuclein are available for cross-linking by tTG. A higher probability for intramolecular cross-linking implies a commensurately smaller probability of formation of intermolecular cross-links. In such a situation, all available sites will be rapidly modified, resulting in only

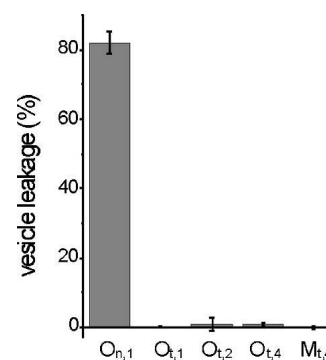


**Figure 4.** Vesicle permeabilization assay. O<sub>n,1</sub>: Normal  $\alpha$ -synuclein oligomers used at 1  $\mu$ M; O<sub>t,1</sub>, O<sub>t,2</sub>, and O<sub>t,4</sub>: SEC purified 1.3  $\mu$ M tTG/ $\alpha$ -synuclein oligomers used at 1, 2, and 4  $\mu$ M, respectively. M<sub>t,4</sub>: SEC purified 1.3  $\mu$ M tTG/ $\alpha$ -synuclein monomers used at 4  $\mu$ M.

small oligomers, which may be efficiently cleared by the intracellular degradation systems. We speculate that oligomer formation may be the predominant process early in PD, while at later stages, with higher tTG and  $\alpha$ -synuclein concentrations (Rockenstein et al. 2001; Muma 2007) the probability of intermolecular cross-linking and formation of large, insoluble protein clusters increases.

SEC analysis of the reaction products revealed that even at micromolar tTG concentrations the predominant products are intramolecularly cross-linked monomers together with a smaller fraction of oligomers. At physiological conditions inside neurons,  $\alpha$ -synuclein concentration is estimated to be 70 to 140  $\mu$ M (Lodish 2000; Schultz 2006), while the neuronal tTG concentration has been reported to be in the nanomolar range (Konno et al. 2005b). Thus intramolecularly cross-linked  $\alpha$ -synuclein is likely the main reaction product of tTG cross-linking in vivo, consistent with the observation of highly enriched intramolecularly cross-linked  $\alpha$ -synuclein monomers together with a small fraction of oligomers in PD *substantia nigra* compared to control tissue (Andringa et al. 2004). Particularly interesting is the good correspondence between the in vivo findings and our in vitro results.

CD spectroscopy revealed that, although the tTG/ $\alpha$ -synuclein oligomers are unstructured, cross-linked protein assemblies, they are still competent to fold into an  $\alpha$ -helix conformation upon binding SDS. Investigations on tTG cross-linking of the non-A $\beta$  component (NAC) of Alzheimer's disease amyloid, which is identical to the NAC region of  $\alpha$ -synuclein, showed that intramolecular cross-links are formed between the glutamine residue at position 79 and the lysine at position 80 (Jensen et al. 1995). In  $\alpha$ -synuclein, however, glutamine and lysine residues outside the NAC region may participate in formation of multiple cross-links. The N-terminal part of  $\alpha$ -synuclein is known to be involved in  $\alpha$ -helix formation in the presence of SDS or upon binding to lipid vesicles (Bussell Jr. et al. 2005). The ability of tTG/ $\alpha$ -synuclein monomers, containing only intramolecular cross-links, to adopt  $\alpha$ -helix conformation suggests that any cross-links formed in the N-terminal region do not interfere with the ability to form helical structure, but nonetheless inhibit folding into  $\beta$ -sheet containing structures (Figs. 2, 3).

On-pathway oligomeric intermediates of  $\alpha$ -synuclein formed during aggregation are currently considered as the most likely toxic species, operating by disrupting cellular membranes (Volles et al. 2001). The exact mechanism of toxicity of these oligomers is unclear. Although our vesicle permeabilization data suggest that the tTG-cross-linked  $\alpha$ -synuclein oligomers are nontoxic, further investigations will be required to study the toxicity in a cell assay. The absence of secondary structure in the tTG/ $\alpha$ -synuclein oligomers and their inability to disrupt membranes indicates that normal oligomers contain structural

elements essential for the disruption process. Indeed, normal oligomers have a considerable content of  $\beta$ -sheet and  $\alpha$ -helical motifs (Fig. 3D), consistent with previous reports (Eliezer et al. 2001). Thus, it appears that the multiple cross-links likely present within the tTG/synuclein oligomers modulate secondary structure, rendering the tTG oligomers incapable of disrupting membranes (Fig. 4).

Further study will be required to evaluate the relevance of both intra- and intermolecular tTG cross-linking in view of disease progression and for the development of viable pharmacological strategies targeting tTG (Wilhelmus et al. 2008).

## Materials and Methods

### *Production of recombinant $\alpha$ -synuclein*

Recombinant expression and purification of human wild-type and A30P, E46K, and A53T disease mutant  $\alpha$ -synuclein was performed as described previously (van Raaij et al. 2006).

### *SEC, SDS-PAGE, and native PAGE*

SEC was performed using an Åkta Basic system equipped with a Superdex 200 column (GE Healthcare). Elution was monitored by 275-nm absorbance using 10 mM Tris-HCl, 50 mM NaCl, pH 7.4 elution buffer at a flow rate of 0.5 mL/min. SDS-PAGE using 15% and 16.5% polyacrylamide gels and native PAGE with 3.5% to 17% continuous gradient polyacrylamide gels was performed.

### *Surface plasmon resonance (SPR)*

SPR experiments were performed using a BIAcore 2000 (GE Healthcare) biosensor instrument. Sensor chips and protein coupling chemicals were purchased from BIAcore AB. Wild-type, A30P, E46K, and A53T  $\alpha$ -synuclein were coupled to the surface of the sensor flow cell as described previously (Wilhelmus et al. 2006). Kinetic measurements were performed at 25°C with a flow rate of 10  $\mu$ L/min in 10 mM HEPES, pH 7.4, 150 mM NaCl, 3 mM EDTA, 0.005% (v/v) surfactant P20. Interaction of tTG with  $\alpha$ -synuclein was monitored using six different tTG concentrations (0.32–2.6  $\mu$ M). The sensor surface was regenerated with 20  $\mu$ L of 10 mM NaOH. The BIAcore kinetic evaluation software was used to generate overlay plots of the six analyte concentrations to determine the relative dissociation constants ( $K_D$ ). All experiments were performed in duplicate per chip, and at least two different sensor chips were used to exclude chip-to-chip variations. See the Supplemental material for a more detailed description of the SPR experiments.

### *Aggregation reactions*

Monomeric  $\alpha$ -synuclein variants were incubated at 100  $\mu$ M in 10 mM Tris-HCl, 50 mM NaCl, 5 mM CaCl<sub>2</sub>, 10 mM DTT, pH

7.4 at 37°C under constant shaking. Different guinea pig liver tissue transglutaminase (Sigma) concentrations were included in the incubations as indicated in the figure legends. Aggregation kinetics were monitored by dilution in 5  $\mu$ M Thioflavin T (ThioT) solution in 10 mM Tris-HCl, pH 7.4 at specific time points (van Raaij et al. 2006).

#### Preparation of oligomeric $\alpha$ -synuclein

Oligomers were prepared by drying 250  $\mu$ M  $\alpha$ -synuclein stock solution in 10 mM Tris-HCl, pH 7.4 in a vacuum evaporator, redissolving at 1 mM in MilliQ water, and shaking at 1250 rpm for 18 h at room temperature. Oligomers were purified on a Superdex 200 size-exclusion column (GE Healthcare) in 10 mM Tris, 150 mM NaCl, pH 7.4. Protein concentration was determined from 275-nm absorption after correction for scattering contributions (Bendit and Ross 1961).

#### Atomic force microscopy (AFM)

For AFM measurements aggregation aliquots were diluted in 10 mM Tris, 50 mM NaCl, pH 7.4, adsorbed onto mica, washed twice with 50  $\mu$ L MilliQ water, and gently dried under nitrogen gas. Tapping mode AFM height images were made on a custom-built instrument (van der Werf et al. 1993). SPIP software (Image Metrology A/S) was used to analyze images. See the Supplemental material for a more detailed description of the AFM experiments.

#### Vesicle permeabilization assay

A 10- $\mu$ L aliquot of 10 mg/mL 1-palmitoyl, 2-oleoyl phosphatidylglycerol (POPG) (Avanti Polar Lipids, Inc.) stock solution in chloroform was dried gently using nitrogen gas followed by 4 h drying under vacuum. The lipid film was rehydrated to an osmolarity of 330 mOsm in 10 mM HEPES, pH 7.4 buffer containing 50 mM calcein (Sigma) and NaCl for 1 h with brief agitation every 10 min. After 5 freeze-thaw cycles using liquid nitrogen, the solution was extruded through a 100-nm pore size polycarbonate membrane filter. Free dye was removed on a G100 Sephadex gel filtration column (GE Healthcare) and phospholipid concentration of the calcein-filled large unilamellar vesicles (LUVs) was determined (Chen et al. 1956). In the permeabilization assay 40  $\mu$ M phospholipid containing vesicle solution was mixed 1:1 (v/v) with  $\alpha$ -synuclein solution and incubated for 30 min at room temperature. Fluorescence (emission: 505 to 550 nm, excitation: 494 nm) was measured using a Cary Eclipse spectrofluorimeter (Varian Inc.). From the background-corrected fluorescence, the vesicle leakage was calculated relative to maximum vesicle disruption induced by 0.5% (w/v) Triton X-100.

#### Circular dichroism spectroscopy

Far-UV CD spectra were recorded on a Jasco J-715 spectropolarimeter (JASCO) operated at room temperature using a 0.5 mm path length quartz cuvette. Spectra were recorded from 190 to 250 nm and corrected for background absorption. Protein concentration was 20  $\mu$ M.

#### Electronic supplemental material

The Supplemental material consists of three figures: Figure S1, quantitative SDS-PAGE analysis of tTG/ $\alpha$ -synuclein cross-linking; Figure S2, native PAGE of tTG/ $\alpha$ -synuclein fractions from SEC; and Figure S3, CD spectra.

#### Acknowledgments

The authors thank Kirsten van Leijenhof-Groener, Yvonne Kraan, and Marloes ten Haaff-Kolkman for assistance in protein production, and Kees van der Werf for AFM support. G.V. was supported by the Stichting Internationaal Parkinson Fonds. This work is part of the research program of the "Stichting voor Fundamenteel Onderzoek der Materie" (FOM), which is supported by the "Nederlandse Organisatie voor Wetenschappelijk Onderzoek" (NWO).

#### References

- Andringa, G., Lam, K.Y., Chegary, M., Wang, X., Chase, T.N., and Bennett, M.C. 2004. Tissue transglutaminase catalyzes the formation of  $\alpha$ -synuclein crosslinks in Parkinson's disease. *FASEB J.* **18**: 932–934.
- Bendit, E.G. and Ross, D. 1961. A technique for obtaining the ultraviolet absorption spectrum of solid keratin. *Appl. Spectros.* **15**: 103–105.
- Bussell Jr., R., Ramlall, T.F., and Eliezer, D. 2005. Helix periodicity, topology, and dynamics of membrane-associated  $\alpha$ -synuclein. *Protein Sci.* **14**: 862–872.
- Chen, P.S., Toribara, T.Y., and Warner, H. 1956. Microdetermination of phosphorus. *Anal. Chem.* **28**: 1756–1758.
- Eliezer, D., Kutluay, E., Bussell Jr., R., and Browne, G. 2001. Conformational properties of  $\alpha$ -synuclein in its free and lipid-associated states. *J. Mol. Biol.* **307**: 1061–1073.
- Jensen, P.H., Sørensen, E.S., Petersen, T.E., Gliemann, J., and Rasmussen, L.K. 1995. Residues in the synuclein consensus motif of the  $\alpha$ -synuclein fragment, NAC, participate in transglutaminase-catalyzed cross-linking to Alzheimer-disease amyloid  $\beta$ A4 peptide. *Biochem. J.* **310**: 91–94.
- Junn, E., Ronchetti, R.D., Quezado, M.M., Kim, S.Y., and Mouradian, M.M. 2003. Tissue transglutaminase-induced aggregation of  $\alpha$ -synuclein: Implications for Lewy body formation in Parkinson's disease and dementia with Lewy bodies. *Proc. Natl. Acad. Sci.* **100**: 2047–2052.
- Kim, S.-Y., Grant, P., Lee, J.H., Pant, H.C., and Steinert, P.M. 1999. Differential expression of multiple transglutaminases in human brain. Increased expression and cross-linking by transglutaminases 1 and 2 in Alzheimer's disease. *J. Biol. Chem.* **274**: 30715–30721.
- Konno, T., Morii, T., Hirata, A., Sato, S., Oiki, S., and Ikura, K. 2005a. Covalent blocking of fibril formation and aggregation of intracellular amyloidogenic proteins by transglutaminase-catalyzed intramolecular cross-linking. *Biochemistry* **44**: 2072–2079.
- Konno, T., Morii, T., Shimizu, H., Oiki, S., and Ikura, K. 2005b. Paradoxical inhibition of protein aggregation and precipitation by transglutaminase-catalyzed intermolecular cross-linking. *J. Biol. Chem.* **280**: 17520–17525.
- Lashuel, H.A., Petre, B.M., Wall, J., Simon, M., Nowak, R.J., Walz, T., and Lansbury Jr., P.T. 2002.  $\alpha$ -Synuclein, especially the Parkinson's disease-associated mutants, forms pore-like annular and tubular protofibrils. *J. Mol. Biol.* **322**: 1089–1102.
- Lodish, H.F. 2000. *Molecular cell biology*, 4th ed. Freeman, New York.
- Miller, M.L. and Johnson, G.V. 1995. Transglutaminase cross-linking of the  $\tau$  protein. *J. Neurochem.* **65**: 1760–1770.
- Muma, N.A. 2007. Transglutaminase is linked to neurodegenerative diseases. *J. Neuropathol. Exp. Neurol.* **66**: 258–263.
- Murtaugh, M.P., Arend, W.P., and Davies, P.J. 1984. Induction of tissue transglutaminase in human peripheral blood monocytes. *J. Exp. Med.* **159**: 114–125.
- Rockenstein, E., Hansen, L.A., Mallory, M., Trojanowski, J.Q., Galasko, D., and Masliah, E. 2001. Altered expression of the synuclein family mRNA in Lewy body and Alzheimer's disease. *Brain Res.* **914**: 48–56.
- Schults, C.W. 2006. Lewy bodies. *Proc. Natl. Acad. Sci.* **103**: 1661–1668.
- Spillantini, M.G., Schmidt, M.L., Lee, V.M., Trojanowski, J.Q., Jakes, R., and Goedert, M. 1997.  $\alpha$ -Synuclein in Lewy bodies. *Nature* **388**: 839–840.

- van der Werf, K.O., Putman, C.A.J., de Grooth, B.G., Segerink, F.B., Schipper, E.H., van Hulst, N.F., and Greve, J. 1993. Compact stand-alone atomic force microscope. *Rev. Sci. Instrum.* **64**: 2892–2897.
- van Raaij, M.E., Segers-Nolten, I.M., and Subramaniam, V. 2006. Quantitative morphological analysis reveals ultrastructural diversity of amyloid fibrils from  $\alpha$ -synuclein mutants. *Biophys. J.* **91**: L96–L98. doi: 10.1529/biophysj.106.090449.
- Volles, M.J., Lee, S.J., Rochet, J.C., Shtilerman, M.D., Ding, T.T., Kessler, J.C., and Lansbury Jr., P.T. 2001. Vesicle permeabilization by protofibrillar  $\alpha$ -synuclein: Implications for the pathogenesis and treatment of Parkinson's disease. *Biochemistry* **40**: 7812–7819.
- Wilhelmus, M.M., Boelens, W.C., Otte-Höller, I., Kamps, B., de Waal, R.M., and Verbeek, M.M. 2006. Small heat shock proteins inhibit amyloid- $\beta$  protein aggregation and cerebrovascular amyloid- $\beta$  protein toxicity. *Brain Res.* **1089**: 67–78.
- Wilhelmus, M.M., van Dam, A.-M., and Drukarch, B. 2008. Tissue transglutaminase: A novel pharmacological target in preventing toxic protein aggregation in neurodegenerative diseases. *Eur. J. Pharmacol.* **585**: 464–472.